JOURNAL OF SOLID STATE CHEMISTRY 118, 285–291 (1995)

New Ni–Al–Cr and Ni–Al–Fe Carbonate Hydrotalcite-like Compounds: Synthesis and Characterization

F. Kooli,[1] K. Kosuge, and A. Tsunashima

Materials Processing Department, National Institute for Resources and Environment, 16-3 Onogawa, Tsukuba, 305 Japan

Received December 15, 1994; in revised form April 25, 1995; accepted April 27, 1995

A series of Ni–Al–M (M = Cr or Fe) double-hydroxide phases with carbonate anions were prepared by coprecipitation, at 60°C, of the corresponding chloride and nitrate solutions with sodium carbonate aqueous solution at pH 10, followed by hydrothermal treatment at 150°C. The characterization and the thermal stability properies of the products were also investigated. Pure hydrotalcite-like materials are obtained, unless an excess of Al or Fe is used, in such a case, an additional phase of pseudoboemite or iron oxide, respectively, is also obtained. Incorporation of aluminum ions in the host layer depends on the nature of the coexistent trivalent cation (chromium or iron), and the thermal stability at high temperatures also depends on the nature of the trivalent cation. © 1995 Academic Press, Inc.

INTRODUCTION

Hydrotalcite-like (HT) compounds, which are referred to as anionic clays, have the general chemical formula $[M_{1-x}M'_x(OH)_2]A^{n-}_{x/n}mH_2O$, where M is a divalent cation such as Mg, Zn, Ni, ..., M' is a trivalent cation such as Al, Cr, Fe, ...; A^{n-} is an anion like Cl^-, NO_3^-, SO_4^{2-}, CO_3^{2-}, ..., (the latter usually being the most common); the x lies in the range 0.20–0.33 (1, 2, 3). These compounds have a positively charged brucite-like hydroxide layer, resulting from the substitution of a divalent by a trivalent cation. The positive charge is compensated by an exchangeable interlayer anion, and water molecules are intercalated between the layers (4). Zinc-aluminum HT compounds with x in the range 0.33–0.44 have also been obtained (5). The general formula could also be extended to include a monovalent cation in the octahedral sites (6).

HT compounds have been found to have many practical applications, including as anion exchangers in catalysis and as supports for the controlled release of biologically active molecules (7). Interesting properties of the oxides which are obtained by calcination include high surface areas and surface basic characteristics. Calcination also results in the formation of homogeneous mixtures of oxides with very small crystal size which are stable to thermal treatments, and which by reduction, form small and thermally stable mental crystalites. High surface area Ni/Al mixed oxides resulting from thermal decomposition of Ni–Al HTs have been investigated as catalyst precursors on account of the interesting properties of the final catalyst, including high metallic dispersion and particle stability (7).

The resistance of Ni–Al catalysts toward steam sintering can be improved by introducing a trivalent cation into the precursor substitute for aluminum (8). It was claimed that the substitution of aluminum gave rise to calcined catalysts with increased pore volumes and pore radius. This property was reported to be beneficial in regards to the improvement of catalytic performance.

We have previously reported on several Mg–Zn–Al hydroxide sulfate compounds with the HT structure (9). However, so synthesis of HT systems with one divalent cation and two trivalent cations per empirial formula has been reported. In the present study, different Ni–Al–Cr and Ni–Al–Fe hydroxide carbonate compounds were synthesized, and the influence of the M/Al and Ni/(Al + M) ratios (M = Cr or Fe) on the phases obtained were investigated. Chemical analysis, powder X-ray diffraction, Fourier transform infra-red spectroscopy, and thermal data are also reported.

EXPERIMENTAL

Preparation of Samples

The two double hydroxy-carbonate layered systems were prepared as described previously (9). The Ni–Al–M ($M = Fe^{3+}$, Cr^{3+}) solid solutions were formed by coprecipitation at 60°C from chromium or iron chloride and nickel and aluminium nitrate solutions, added dropwise by pumps into 100 ml of 1 M sodium carbonate aqueous solution, with constant stirring. The pH was kept constant at 10 by addition of a 3 M sodium hydroxide solution. The coprecipitates were aged in their mother liquors at

[1] Present address: Department of Chemistry, University of Cambridge, Lensfield Road, Cambridge CB2 1EW, UK.

0022-4596/95 $12.00

TABLE 1
Chemical Analysis Results of the Powders and Lattice Parameters of the HT Structure Phase in the Ni–Al–Cr System

S	Cr/Al[a]		Ni/(Cr + Al)[a]		Phase[b]	Unit cell parameters	
	Theo	Exp	Theo	Exp		a (Å)	c (Å)
A1	0	0	1.12	1.21	HT, (PB)	3.016	22.410
A2	0	0	2.22	2.58	HT, (PB)	3.028	22.722
A3	0	0	3.36	3.60	HT	3.046	23.358
C1	0.11	0.10	1.10	1.10	HT, (PB)	3.018	22.074
C2	0.11	0.11	2.20	2.43	HT, (PB)	3.034	23.060
C3	0.11	0.11	3.28	3.71	HT	3.042	23.280
C4	0.11	0.13	4.40	4.88	HT	3.052	23.460
C5	0.11	0.12	6.63	6.78	HT	3.064	24.022
C6	0.78	0.96	1.05	1.15	HT, (PB)	3.020	22.692
C7	1.13	1.93	3.18	4.19	HT, (PB)	3.042	23.358
C8	1.11	2.02	4.18	5.52	HT, (PB)	3.054	23.050
C9	1.11	1.56	6.25	6.85	HT, (PB)	3.070	23.592
C10	0.22	0.20	2.20	2.28	HT	3.038	23.070
C11	0.56	0.60	2.16	2.50	HT, (PB)	3.038	23.058
C12	2.23	1.63	2.07	2.33	HT, (PB)	3.050	23.080
C13	4.40	1.63	2.04	2.62	HT, (PB)	3.054	23.080
C14	6.70	5.62	2.04	2.77	HT, (PB)	3.056	22.950
C15	8.80	6.59	2.02	3.02	HT, (PB)	3.058	23.040
C16	11.1	5.40	2.02	3.53	HT, (PB)	3.058	23.060

Note. S, sample name; Theo, theoretical; Exp, experimental; HT, hydrotalcite; (PB), traces of pseudoboemite.
[a] Atomic ratio.
[b] As detected by PXRD.

60°C for 1 hr, then filtered and washed with 1 liter of boiling distilled water, and dried at 50°C for 24 hr. One-half gram of the dried precipitates were suspended in 10 ml of distilled water, in a Teflon cell, for hydrothermal treatment by autogeneous pressure at 150°C for 12 hr. The sample was then filtered, washed with water, and dried at 50°C overnight.

Analysis and Measurements

The amounts of the Ni^{2+}, Al^{3+}, Cr^{3+}, or Fe^{3+} in the products were determined by X-ray fluorescence (XRF), with a Rigaku Geigerflex IKF, X-ray spectrometer. For the characterization of the phases obtained and the determination of the unit cell parameters, a Rigaku RU300 equipped with Cu$K\alpha$ radiation and a nickel filter was used. Simultaneous thermogravimetry (TG) and differential thermal analyses (DTA) were carried out with a Rigaku apparatus, at a heating rate of 15°C/min, in air, using 5–6 mg of sample. Fourier transform infrared (FTIR) spectra were recorded in a JEOL JIR 3510 FTIR spectrometer, using a small amount of sample mixed with KBr, in the 4000–400 cm^{-1} range. The thermal properties studies were performed on 0.5 g of sample calcined in air for 2 hr, at various temperatures in the range 200–1000°C, in a Thermolyne 10500 furnace.

RESULTS AND DISCUSSION

Chemical Analysis

The results for the Ni–Al–Cr system with various Cr/Al and Ni/(Al + Cr) are reported in Table 1 and Fig. 1. In the case of Ni–Al solid solutions (samples A1–A3), the experimental values of the Ni/Al ratios are higher than those theoretically expected, which means that aluminum is not completely precipitated. Clause *et al.* found that all cations are completely precipitated in the same system at different experimental conditions (16).

In the Ni–Al–Cr system, with low chromium content (samples C1–C5), the experimental and theoretical values of Cr/Al almost coincide, the experimental Ni/(Al + Cr) ratios are higher than the theoretical ones, except for Ni/(Al + Cr) = 5 (sample C5), where the value is smaller, showing that the aluminum content in the coprecipitate is lower than expected.

When the Cr/Al ratio increases (Cr/Al ≈ 1.10, samples C6–C9), the experimental values of Cr/Al and Ni/(Al +

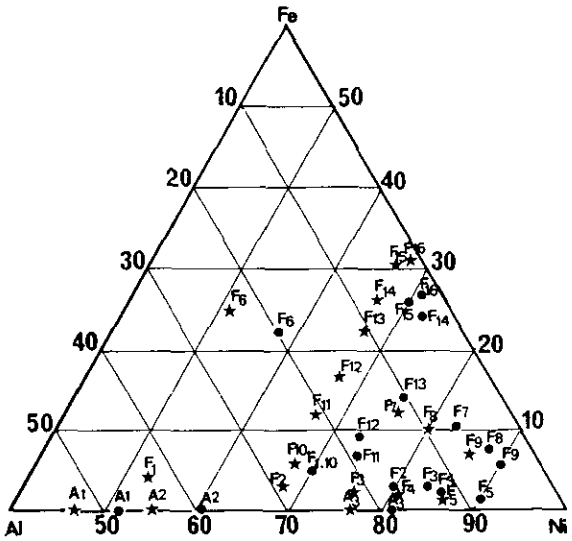

FIG. 1. Theoretical (●) and experimental (★) chemical composition of the powders as presented on an Ni–Al–Cr (atomic percentage).

Cr) are always higher than the theoretical ones. These results show that aluminum is not completely precipitated. For Ni/(Al + Cr) = 2 and $0.2 \leq Cr/Al \leq 11$, the experimental values of Cr/Al are, however, smaller than the theoretical ones when $Cr/Al > 1.0$ (samples C12–C16). The experimental ratios of Ni/(Al + Cr) are always higher than the theoretical ratios. The XRF analysis showed in this case a large variation in the chromium content in the solid solution, as compared to that of the liquid solutions, which is not the case for aluminum. This fact can be due to a lower reactivity of chromium ions compared to aluminum, during coprecipitation.

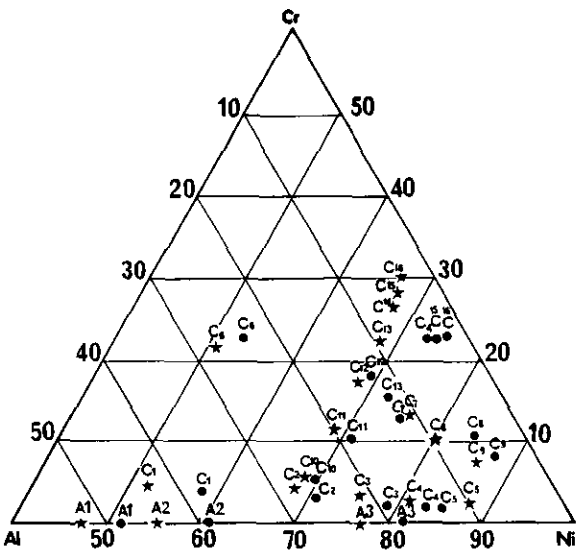

FIG. 2. Theoretical (●) and experimental (★) chemical composition of the powders as presented on an Ni–Al–Cr (atomic percentage).

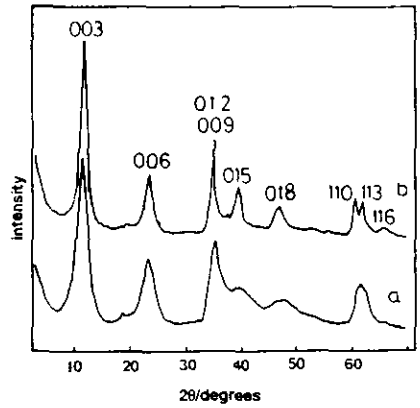

FIG. 3. PXRD patterns of sample C2: (a) untreated, (b) after hydrothermal treatment.

The chemical analysis results for the Ni–Al–Fe system are shown in Table 2 and Fig. 2. Whatever the quantity of iron added, the Fe/Al and Ni/(Al + Fe) experimental ratios are always higher than the theoretical ones (samples F1–F16). This behavior is due to the lower reactivity of aluminum during coprecipitation.

Summarizing these results, the behavior of the aluminum ion seems to depend on the nature of the other trivalent cation. In the Ni–Al–Cr system, at high chromium content, the aluminum cation has good reactivity during coprecipitation. However, in the Ni–Al–Fe system, its reactivity is lower than that of iron.

X-Ray Diffraction

Hydrothermal treatment improved the crystallization of these compounds, and a typical PXRD pattern of carbonate HT compounds was obtained (Fig. 3). So all the values of the unit cell parameters, assuming rhombohedral symmetry, with the c parameter corresponding to three times the thickness of the expanded brucite-like layer, are included in Tables 1 and 2 for the Ni–Al–Cr and Ni–Al–Fe systems, respectively, after hydrothermal treatment. The qualitative crystallographic compositions of the samples are also listed in these tables.

In the Ni–Al system, the samples exhibit the hydrotalcite structure only, except when the Ni/Al ratio was smaller than 2, where a small amount of pseudoboehmite was detected (samples A1, A2). The values of parameters a and c decrease when the aluminum content increases. This fact can be explain by substitution of the larger Ni^{2+} ions by smaller Al^{3+} ions (10), and by the increase of the electrostatic bonding between the positive brucite-like layers and the negative interlayer anions (11, 12).

For low chromium content, a small amount of pseudoboehmite phase was also detected if Ni/(Al + Cr) < 2 (samples C1, C2). The a and c parameters decrease when

TABLE 2
Chemical Analysis Results of the Powders and Lattice Parameters of the HT Structure Phase in the Ni–Al–Fe System

	Fe/Al[a]		Ni/(Fe + Al)[a]			Unit cell parameters	
S	Theo	Exp	Theo	Exp	Phase[b]	a (Å)	c (Å)
A1	0	0	1.12	1.21	HT, (PB)	3.016	22.410
A2	0	0	2.22	2.58	HT, (PB)	3.028	22.722
A3	0	0	3.36	3.60	HT	3.046	23.358
F1	0.11	0.18	1.10	2.30	HT	3.022	22.560
F2	0.11	0.17	2.22	3.86	HT	3.048	23.262
F3	0.11	0.21	3.32	5.09	HT	3.052	23.422
F4	0.11	0.17	4.43	6.01	HT	3.056	23.490
F5	0.11	0.18	6.57	9.87	HT	3.060	23.352
F6	1.12	1.15	1.05	1.35	HT, IO	3.030	22.800
F7	1.12	1.68	3.16	3.36	HT	3.054	23.400
F8	1.11	1.44	4.21	7.46	HT	3.064	23.484
F9	1.13	1.68	6.32	9.79	HT	3.076	23.265
F10	0.22	0.30	2.19	2.91	HT, (IO)	3.038	23.884
F11	0.56	0.59	2.15	2.83	HT, (IO)	3.046	22.914
F12	1.11	1.42	2.11	3.17	HT	3.046	22.932
F13	2.21	2.58	2.00	2.66	HT, IO	3.070	23.220
F14	4.19	8.25	2.02	2.64	HT, IO	3.070	23.070
F15	6.75	10.35	2.03	2.62	HT, IO	3.058	23.070
F16	10.93	16.67	2.02	2.21	HT, IO	3.082	23.142

Note. S, sample name; Theo, theoretical; Exp, experimental; HT, hydrotalcite; (PB), traces of pseudoboemite; IO, iron oxide; (IO), traces of IO.

[a] Atomic ratio.

[b] As detected by PXRD.

the content of aluminum increases, and a values are higher in the presence of chromium than the a values in the Ni–Al system.

For higher chromium contents (Cr/Al $\approx$ 1.1), the value of a still decreases. A pseudoboehmite phase was formed together with the hydrotalcite phase, whatever the Ni/(Al + Cr) ratio (samples C6–C9). The high value of the a parameter is probably due to the larger ionic radius of chromium, when compared to that of aluminium.

When Ni/(Al + Cr) $\approx$ 2 and the Cr/Al ratio changes from 0.2 to 11, substitution of aluminum by chromium affects only very slightly the value of a, which varies from 3.038 to 3.058 Å, while c remains close to 23.05 Å (samples C10–C16).

In the case of the Ni–Al–Fe system (Table 2), with a low iron content, the samples obtained are pure hydrotalcite, except for Ni/(Al + Fe) = 1 (sample F1), where traces of pseudoboehmite phase were also detected. The increase of a and c can be related to the decrease in the aluminum content in the solid solution, but both a and c values are higher than for the Ni–Al system.

When Fe/Al ratio $\approx$ 1.1, the values of a and c increase, when the trivalent cation content decreases. An iron oxide phase (Fe_2O_3) was formed together with HT compounds at Ni/(Al + Fe) $<$ 2 (samples F6–F9). The increase of the a value compared to the a value in the Ni–Al system is probably due to the large ionic radius of iron compared to aluminum.

When substitution of aluminum by iron increases ($0.2 \leq$ Fe/Al ≤ 11), the value of the a varies from 3.038 to 3.082 Å (samples F10–F16). In all cases, an iron oxide phase was also formed together with the hydrotalcite, and the intensity of the iron oxide peaks increases with the increase in the iron content in the starting solution. As in the case of Ni–Al–Cr, the c value is also affected by the content of the intercalated water molecules, which influence the orientation of the interlayer carbonate anions (13).

Thermogravimetric Analysis

The diagrams are quite similar to those of natural hydrotalcite (14). The weight loss for the Ni–Al (sample A2) and Ni–Al–Cr systems takes place in two steps. From the temperature range where these effects are recorded, the first one corresponds to the loss of the physically adsorbed and interlayer water. The second is due to the loss of CO_2 from the layers and to the dehydroxylation

of the brucite-layers (15). However, when the chromium content increases (sample C13), a small and continuous weight loss is observed in the range 450–500°C. This step can be due to the complete elimination of the carbonate anion (16). However, recently a similar step was attributed to removal of O_2 during reduction of the Cr(VI) to Cr(III) formed during the thermal treatment (17, 18).

Each weight loss is accompanied by an endothermic transformation. The loss of physically adsorbed water is accompanied by a broad endothermic peak around 70°C. The peak between 150–180°C is attributed to the loss of interlayer water, but the temperature range is smaller than in the Ni–Al system. Dehydroxylation of the brucite-like layer and removal of CO_2 corresponds to the endothermic peak in the range 300–350°C. The substitution of aluminum by chromium does not affect the temperature of this peak, which is shifted to 350°C only when the content of trivalent cations decreases.

For some DTA curves, a broad endothermic peak around 280–300°C was recorded. This peak was attributed to the dehydroxylation of crystalline $Ni(OH)_2$ phase (19), but this is not the case with our samples, since $Ni(OH)_2$ is not detected by XRD. This peak is probably due the loss of structural water bound to Al ions in the main layer (20) and/or to the partial dehydroxylation of the brucite-like layers (3).

As with the Ni–Al–Cr system, the TG diagram for the Ni–Al–Fe system showed two weight losses and a smaller one, at relatively high temperatures. The first step is attributed to the loss of the adsorbed and interlamelar water, and it also corresponds to the broad endothermic peak around 70°C, and to the first endothermic peak around 180–220°C. The second step is caused by the loss of hydroxyl groups and CO_2 between the brucite layers, and is accompanied by the second endothermic peak in the range 300–340°C. The smaller weight loss at relatively high temperatures, in the range 500–600°C, is attributed to the complete elimination of the remaining carbonate anions. It is not accompanied by any endothermic peak (sample F7).

When the Fe/Al is smaller than 1.1, another endothermic peak around 275–300°C is observed; as described above, it is attributed to the partial dehydroxylation of the brucite layers. When the substitution of aluminum by iron increases, the temperature of the second endothermic peak is shifted to lower temperatures. This means that not all the iron is incorporated in the brucite layer, so the electrostatic interaction between the carbonate anions and the brucite layer is weaker. In this case, PXRD also showed the formation of iron oxide.

Fourier Transform Infrared Spectroscopy

The spectra of the Ni–Al system (Fig. 4a) show a strong absorption band in the range 3530–3440 cm^{-1}, attributed

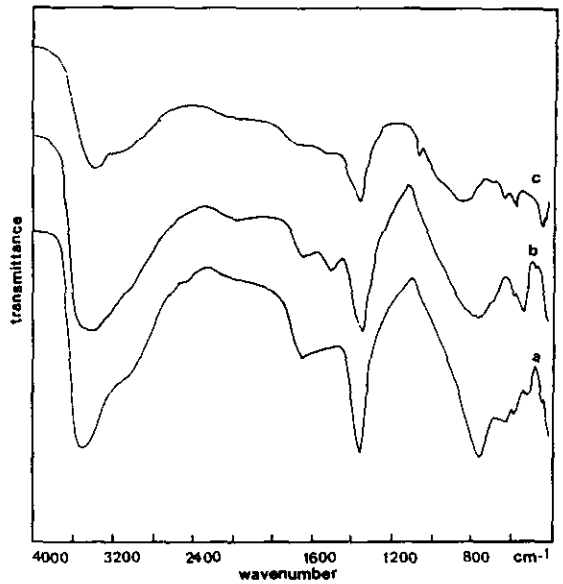

FIG. 4. FTIR spectra of the products: (a) sample A2, (b) sample C15, (c) sample F15.

to the wavenumber vibration of the OH group (δ(OH)), with its position shifted to the higher wavenumber region because of the decrease of aluminium in the hydrotalcite. This shift should be due to a lower electron density of the O–H bond in hydroxyl groups bonded to Al(III) cations. The shoulder around 3100–3000 cm^{-1} is assigned to hydrogen bonding between H_2O molecules and the CO_3^{2-} anions in the interllamelar layer (21, 22). An H_2O bending vibration is also detected around 1630 cm^{-1}.

The ν_3 mode of the CO_3^{2-} anion appears around 1370 cm^{-1}, shifted also to the higher wavenumber range with the decrease in the aluminum content in the brucite layer. In the case of an Ni/Al ratio smaller than 2, the lowering of the symmetry of the carbonate anion leads to a split of the ν_3 band, and also causes the activation of the ν_1 mode of the CO_3^{2-} anion around 1070 cm^{-1}. Similar results were previously obtained (12, 21, 23). The bands around 871 and 670 cm^{-1} are assigned to the ν_2 and ν_4 modes of the carbonate anion, respectively. Other bands which appear around 760 and 557 cm^{-1} may be assigned to vibrations of $[AlO_6]$ unity (24).

With a small quantity of chromium, the $\delta(OH^-)$ and the ν_3 band of CO_3^{2-} shift to higher wavenumbers when the trivalent cation content decreases in the solid solution, and splitting of the ν_3 mode of CO_3^{2-} occurs at Ni/(Al + Cr) < 2. When the substitution of aluminum by chromium increases, it slightly affects the position of the ν_3 band, which shifts from 1360 to 1370 cm^{-1}. The intensities of the bands at 1370 and 1530 cm^{-1} increases simultaneously (Fig. 4b).

For the Ni–Al–Fe system, with a small quantity of iron,

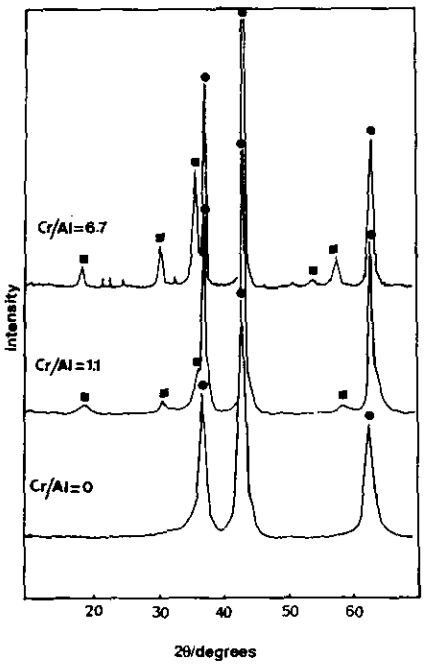

FIG. 5. PXRD patterns of powders at Ni/(Cr + Al) = 2.2 and different Cr/Al ratios calcined at 750°C: (●) NiO, (■) $NiCr_2O_4$.

the position of δ(OH) and the ν_3 mode of (CO_3^{2-}) are slightly shifted to higher wavenumbers, and the intensity of the latter band decreases, with the decrease of the trivalent cation content in the hydrotalcite-like compounds. The shift of the ν_3 mode is also observed at Ni/(Al + Fe) < 2. When the iron content increases, the position of the ν_3 mode of CO_3^{2-} and its intensity seem to be unaffected by the increase in iron content, varying between 1369 and 1365 cm^{-1}. However, the intensity of the band around 1500 cm^{-1} is always weaker than the Ni–Al–Cr system (Fig. 4c).

The position of the ν_3 mode of CO_3^{2-} is not affected by the nature of the trivalent cation, but it seems to be affected by the content of the trivalent cation in the brucite-like layer. The observed shift may be related to the different electronic charge of these layers, indicating an electrostatic interaction between the hydroxyl groups and the carbonate species.

Thermal Properties

In the case of the Ni–Al system (samples A1–A3), at 200°C, removal of interlayer water leads to a decrease of the interlayer distance by about 1 Å. At 300°C, the XRD pattern of the hydrotalcite disappears, and nickel oxide (NiO) phase was detected. Until 850°C, only NiO is detected. The lattice parameters of the nickel oxide formed are smaller than those of pure nickel oxide, indicating the presence of aluminum in the nickel oxide. At temperatures higher than 850°C, a trace of spinel ($NiAl_2O_4$) phase was also detected together with NiO. The amount of spinel phase increases with temperature, but NiO is still the major compound in the calcined products. Formation of the spinel phase is accompanied by a sharpening of the nickel oxide peaks, suggesting a complete decomposition of the nickel-aluminum oxide to nickel oxide and the spinel phase. Similar results were also reported in earlier studies (25, 26).

When the chromium content increases in the solid solution (Cr/Al > 1.1, samples C12–C16), at temperatures around 750°C, the spinel ($NiCr_2O_4$) phase was also detected with the nickel oxide (Fig. 5). At temperatures higher than 750°C, the content of the spinel phase increases, and the nickel oxide was always the major compound.

Compare to the Ni–Al system, the presence of chromium ion in the brucite-like layers decreases the temperature of interaction between the trivalent cation and the nickel oxide, to form a spinel phase at a temperature lower than 750°C.

For the Ni–Al–Fe system, at 750°C, but with a Fe/Al ratio around 0.3 (sample F10), a trace of spinel phase was also detected with the nickel oxide phase, which is not in the case with the Ni–Al–Cr system, where the spinel phase was formed at Cr/Al higher than 1. When the content of iron increases, the spinel ($FeAl_2O_4$) phase was also clearly detected together with NiO (Fig. 6). When the

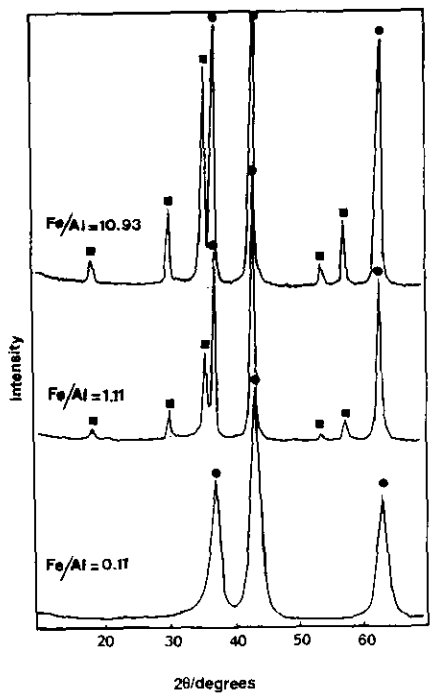

FIG. 6. PXRD patterns of powders at Ni/(Fe + Al) = 2 and different Fe/Al ratios calcined at 750°C: (●) NiO, (■) $NiFe_2O_4$.

temperature increases to about 1000°C, the intensity of the $NiAl_2O_4$ phase peaks increases at a Fe/Al ratio smaller than 0.2 For Fe/Al ratio equal to 1, two spinel phases ($FeAl_2O_4$) and ($NiFe_2O_4$) are also detected, but the first one was more easily identified. For Fe/Al ratios higher than 2, only the $NiFe_2O_4$ phase was detected. However, in all the calcined products, the nickel oxide is the dominant compound.

The presence of iron in the solid solution, even in small amounts, decreases the temperature for formation of the spinel phase, compared to the nickel–aluminum system.

CONCLUSION

In this study, the HT compounds were obtained in both Ni–Al–Cr and Ni–Al–Fe systems with carbonate anions, and the purity of the obtained hydrotalcite depended on the starting composition of the solutions. In the case of the Ni–Al–Fe system, iron oxide was also formed with hydrotalcite in the powders obtained. The reactivity of the aluminum cation also depends on the other coexisting cation, it precipitates easily in the Ni–Al–Cr system, but the precipitation is not complete in the Ni–Al–Fe system.

The thermal properties of the Ni–Al HT compound are affected by the presence of chromium and/or iron ions, at relatively high temperatures, and a spinel phase appears at 750°C, even for small quantities of added iron.

ACKNOWLEDGMENTS

The authors thank Dr T. Kimura from the National Institute for Resources and Environment, Tsukuba, for his assistance in chemical analysis, and Dr J. L. Dubois from the National Chemical Laboratory for Industry, Tsukuba, for helpful discussions and suggestions made concerning this paper. F.K. thanks JISTEC for financial support in the form of a STA fellowship.

REFERENCES

1. M. C. Gaustuche, C. Brown, and M. M. Mortland, *Clay Miner.* **7,** 17 (1967), 177.
2. R. Allmann, *Chimica* **24,** 99 (1970).
3. S. Miyata, *Clays Clay Miner.* **23,** 369 (1975).
4. R. Allman, *Acta. Crystallogr. Sect. B* **24,** 972 (1968).
5. F. Thevnot, R. Szymanski, and P. Chaumette, *Clays Clay Miner.* **37,** 396 (1989).
6. J. C. Serna, J. L. Rendon, and J. E. Iglesias, *Clay. Miner.* **30,** 180 (1982).
7. F. Cavani, F. Trifiro, and A.Vaccari, *Catal. Today* **11,** 173 (1991). [And references therein]
8. C. Komodromos, N. Parkyns, and A. Williams, UK patent 1,550,749 (1977).
9. F. Kooli, K. Kosuge, T. Hibino, and A. Tsunashima, *J. Mater. Sci.* **28,** 2769 (1993).
10. I. Pausch, H. H. Lohse, K. Schurmann, and R. Allmann, *Clays Clay Miner.* **34,** 507 (1986).
11. G. W. Brindley and S. Kikkawa, *Am. Mineral.* **64,** 836 (1979).
12. G. Mascolo and O. Morino, *Mineral. Mag.* **43,** 619 (1980).
13. F. M. Labajos, V. Rives, and M. A. Ulibarri, *Spectrosc. Lett.* **24,** 499 (1991).
14. P. C. Rouxhet and H. F. W. Taylor, *Chimia* **23,** 480 (1969).
15. L. Pesic, S. Salipurovic, V. Markovic, D. Vucelic, W. Kagunya, and W. Jones, *J. Mater. Chem.* **2,** 1069 (1992).
16. O. Clause, M. Gazzano, F. Trifiro, A. Vaccari, and L. Zatroski, *Appl. Catal.* **73,** 217 (1991).
17. F. M. Labajos, *Ph.D. thesis,* Salamanca, Spain, 1993.
18. K. Fuda, K. Suda, and T. Matsunaga, *Chem. Lett.,* 1479 (1993).
19. J. M. Fernandez-Rodriguez, J. Morales, and J. L. Tirado, *J. Mater. Sci.* **21,** 3668 (1986).
20. C. W. Beck, *Am. Mineral.* **35,** 1006 (1950).
21. D. L. Bish and G. W. Brindley, *Amer. Mineralogist.* **62,** 458 (1977).
22. E. C. Kruissink, L. L. Van Reijden, and J. R. H. Ross, *J. Chem. Soc. Faraday Trans. 1* **77,** 649 (1981).
23. M. J. Hernandez-Moreno, M. A. Ulibarri. J. L. Rendon and C. J. Serna. *Phys. Chem. Miner.* **12,** 34 (1985).
24. P. Tarte, *Spectrochem. Acta* **23A,** 2127 (1967).
25. T. Sato, H. Fujita, H. Endo, H. Shimada, and A. Tsunashima, *React. Solids* **5,** 219 (1988).
26. M. J. Hernandez-Moreno, M. A. Ulibarri, J. L. Rendon, and C. J. Serna, *Thermochimica* **81,** 311 (1984).